Check for updates

Received: 16 April 2024 | Revised: 20 August 2024 | Accepted: 31 August 2024

DOI: 10.1111/cas.16343

Cancer Science WILEY

ORIGINAL ARTICLE

Identification of ENO-1 positive extracellular vesicles as a circulating biomarker for monitoring of Ewing sarcoma

Koji Uotani[1] | Tomohiro Fujiwara[1,2] | Koji Ueda[3] | Aki Yoshida[1] | Shintaro Iwata[4] | Takuya Morita[1] | Masahiro Kiyono[1] | Toshiyuki Kunisada[5] | Ken Takeda[6] | Joe Hasei[1] | Yusuke Yoshioka[7] | Takahiro Ochiya[7] | Toshifumi Ozaki[1]

[1]Department of Orthopedic Surgery, Okayama University Graduate School of Medicine, Dentistry, and Pharmaceutical Sciences, Okayama, Japan

[2]Center of Innovative Medicine, Okayama University Hospital, Okayama, Japan

[3]Cancer Precision Medicine Center, Japanese Foundation for Cancer Research, Tokyo, Japan

[4]Department of Musculoskeletal Oncology, National Cancer Center Hospital, Tokyo, Japan

[5]Department of Medical Materials for Musculoskeletal Reconstruction, Okayama University Graduate School of Medicine, Dentistry, and Pharmaceutical Sciences, Okayama, Japan

[6]Department of Intelligent Orthopedic System, Okayama University Graduate School of Medicine, Dentistry, and Pharmaceutical Sciences, Okayama, Japan

[7]Department of Molecular and Cellular Medicine, Institute of Medical Science, Tokyo Medical University, Tokyo, Japan

Correspondence
Tomohiro Fujiwara, Department of Orthopedic Surgery, Okayama University Graduate School of Medicine, Dentistry, and Pharmaceutical Sciences, Okayama, Japan.
Email: tomomedvn@gmail.com and tomomedvn@okayama-u.ac.jp

Funding information
JSPS Kakenhi, Grant/Award Number: 22H03202

Abstract

The lack of circulating biomarkers for tumor monitoring is a major problem in Ewing sarcoma management. The development of methods for accurate tumor monitoring is required, considering the high recurrence rate of drug-resistant Ewing sarcoma. Here, we describe a sensitive analytical technique for tumor monitoring of Ewing sarcoma by detecting circulating extracellular vesicles secreted from Ewing sarcoma cells. Proteomic analysis of Ewing sarcoma cell-derived extracellular vesicles identified 564 proteins prominently observed in extracellular vesicles from three Ewing sarcoma cell lines. Among these, CD99, SLC1A5, and ENO-1 were identified on extracellular vesicles purified from sera of patients with Ewing sarcoma before treatment but not on extracellular vesicles from those after treatment and healthy individuals. Notably, not only Ewing sarcoma-derived extracellular vesicles but also Ewing sarcoma cells demonstrated proteomic expression of CD99 and ENO-1 on their surface membranes. ENO-1$^+$CD63$^+$ extracellular vesicle detection was reduced after tumor resection while both CD99$^+$CD63$^+$ and ENO-1$^+$CD63$^+$ extracellular vesicles were detected in serum from Ewing sarcoma-bearing mice. Finally, the accuracy of liquid biopsy targeting these candidates was assessed using extracellular vesicles from the sera of patients with Ewing sarcoma. Elevated ENO-1$^+$CD81$^+$ extracellular vesicles in the serum of patients before treatments distinguished patients with Ewing sarcoma from healthy individuals with an area under the curve value of 0.92 ($P < 0.001$) and reflected the tumor burden in patients with Ewing sarcoma during multidisciplinary treatments. Collectively, circulating ENO-1$^+$CD81$^+$ extracellular vesicle detection could represent a novel tool for tumor monitoring of Ewing sarcoma.

KEYWORDS
circulating biomarker, Ewing sarcoma, extracellular vesicles, liquid biopsy, proteome

This is an open access article under the terms of the Creative Commons Attribution-NonCommercial License, which permits use, distribution and reproduction in any medium, provided the original work is properly cited and is not used for commercial purposes.
© 2024 The Author(s). *Cancer Science* published by John Wiley & Sons Australia, Ltd on behalf of Japanese Cancer Association.

1 | INTRODUCTION

Ewing sarcoma (ES) is a malignant mesenchymal tumor that develops from bone and soft tissue, predominantly in children and young adults. ES is characterized by prototypical chromosomal translocation and fusion of the *EWS* gene on chromosome 22q24 with one of five E-twenty-six (ETS) transcription factor gene family members (*FLI4*, *ERG5*, *ETV16*, *E1AF7,8*, and *FEV9*).[1] Of the EWS/ETS translocations, 85% of ES harbor the EWS-FLI1 reciprocal translocation t (11;22) (q24;q12).[1] In the past few decades, the detection of fusion gene transcripts and the development of immunohistochemical markers, such as CD99 (MIC2), have helped improve diagnostic accuracy.[2] The current standard treatment for localized ES is a multimodal approach that combines chemotherapy and local therapy consisting of surgery and/or radiotherapy.[3] The 5-year overall survival rate for patients with localized ES approaches 65%–75% because of diagnostic and therapeutic modality development. However, patients with advanced ES demonstrated a dismal prognosis, with a 5-year overall survival of <30%.[4]

The lack of circulating markers for tumor monitoring and prognostic prediction remains a crucial problem in improving patient prognosis. Currently, imaging tests, such as computed tomography and magnetic resonance imaging, are the only useful modality to assess therapeutic response or tumor recurrence. Identifying circulating ES biomarkers may help evaluate the real-time treatment response, detect residual tumors after treatments, and discover recurrent tumors early, which alerts physicians to change to more effective therapies.

Extracellular vesicles (EVs) are a heterogeneous group of cell-derived membranous structures secreted by a multitude of cell types into multiple body fluids, including blood, urine, and saliva.[5] EVs express tetraspanin family proteins (CD9, CD63, and CD81) on their surface[6,7] and contain bioactive cargo (nucleic acids, proteins, and metabolites),[8] which may play a pivotal role in cell–cell communication between tumor cells and the tumor microenvironment.[8] EVs stably exist in the circulation and protect these functional molecules from degeneration caused by hydrolysis.[9] Accumulating evidence has indicated that circulating EVs are a promising biomarker for malignant disease diagnoses.[10–14] Melo et al. revealed that cancer cell-derived EVs expressing glypican-1 distinguished patients with pancreatic cancer from healthy individuals with absolute sensitivity and specificity.[15] Yoshioka et al. determined CD147 and CD9 double-positive EVs as a circulating marker that distinguishes patients with colorectal cancer from healthy individuals and is more accurate than carcinoembrionic antigen (CEA) and carbohydrate antigen 19-9 (CA19-9).[7]

Specific detection and isolation of cancer cell-derived EVs in the circulation in patients with bone sarcoma is currently lacking. This study identified surface markers on ES-derived EVs to develop a method of liquid biopsy as a new modality for tumor monitoring of ES. Surface molecules on the EVs were screened using proteomic analysis using the sera of patients with ES and conditioned media of ES cells. The detection of EVs that target the identified surface marker was evaluated using sera collected from the mouse xenograft model and patients with ES.

2 | MATERIALS AND METHODS

2.1 | Study design

This study consisted of a screening phase and a subsequent validation phase (Figure 1A). In the screening phase, the surface marker proteins of EVs from ES were screened by proteomic analysis using EVs derived from sera of patients with ES and culture media of ES cells. The candidate molecules were selected considering their proteomic expression in the sera of healthy individuals and patients with ES after treatment. In the validation phase, the localization of the surface marker protein on ES-cell-derived EVs was validated using ELISA. Tumor monitoring was then tested using the ES-bearing mouse model by detecting EVs with the identified molecule on their surface membrane. Finally, the accuracy of liquid biopsy targeting EVs with the identified marker on their surface was validated using EVs derived from the sera of patients with ES.

2.2 | Serum collection from patients with ES and ES-bearing mice

Whole-blood samples were obtained from patients with ES and healthy individuals at Okayama University Hospital and Chiba Cancer Center Hospital. Samples were obtained at diagnosis, pre and postoperatively, during chemotherapy, or at disease progression. The local ethics committee approved this study, and all participants signed written informed consent. Murine blood was obtained from cardiac puncture at the indicated time points. Sera were fractionated from whole-blood samples by centrifugation at 2,000*g* for 15 min at 4°C. The collected serum was centrifuged at 20,000 g for 15 min at 4°C, and the supernatants were collected and passed through a 0.22-μm-pore filter (Merck Millipore) and stored at 80°C.

2.3 | Cell lines and cell cultures

This study used human ES cell lines (SK-ES-1, RD-ES, and A673), osteosarcoma (OS) cell lines (143B and HOS), chondrosarcoma (CS) cell lines (OUMS27 and T2147), and human osteoblasts (hOB). SK-ES-1, RD-ES, A673, 143B, and HOS were purchased from the American Type Culture Collection. OUMS27 and T2147 were developed in our laboratory.[16] hOB (Lot#: 3070205) was purchased from PromoCell. These cell lines were cultured in Dulbecco's modified Eagle's medium (DMEM; Gibco Laboratories), Roswell Park Memorial Institute-1640 (Gibco), or Osteoblast Growth Medium

13497006, 0, Downloaded from https://onlinelibrary.wiley.com/doi/10.1111/cas.16343 by Okayama University, Wiley Online Library on [30/09/2024]. See the Terms and Conditions (https://onlinelibrary.wiley.com/terms-and-conditions) on Wiley Online Library for rules of use; OA articles are governed by the applicable Creative Commons License

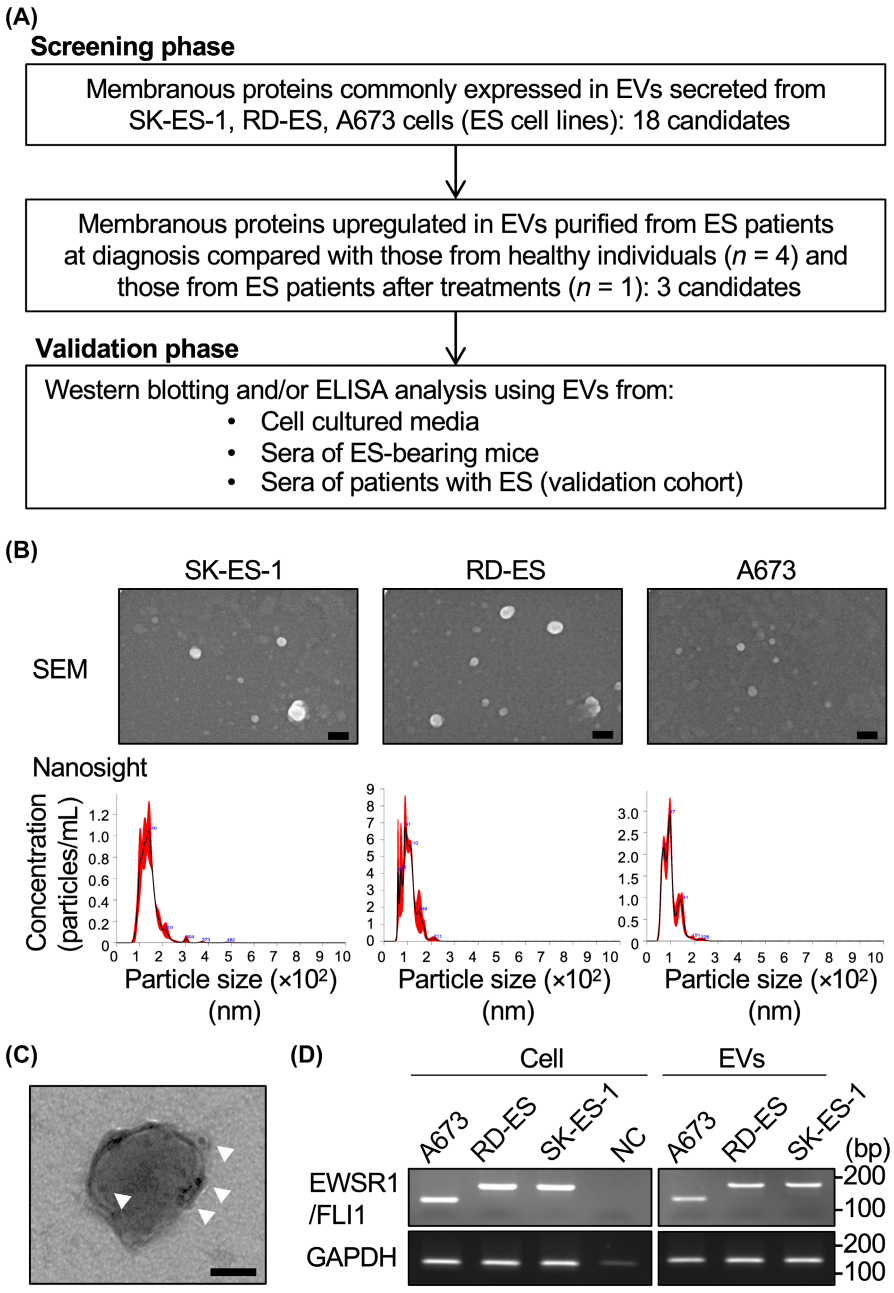

FIGURE 1 Identification and experimental validation of EVs secreted from Ewing sarcoma (ES) cells. (A) The study design. (B) Scanning electron microscopy of pellets obtained after ultracentrifugation of ES cell culture supernatants. The collected EVs were essentially homogeneous and 40–100 nm in diameter. Analysis of the size distribution by the NanoSight® nanoparticle tracking system determined these EVs within approximately 50–150 nm with a peak of 100 nm. (C) Transmission electron microscope with CD81–nanogold for EVs. The collected EVs loaded CD81 tetraspanin protein on their surface (white arrowhead). (D) The fusion gene *EWSR1/FLI-1* transcripts were detected in both ES cell lysates and EVs secreted from ES cell lines. ES, Ewing sarcoma; EVs, extracellular vesicles; SEM, scanning electron microscope.

(PromoCell) supplemented with 10% or 15% fetal bovine serum (FBS; HyClone), 100 units/mL of penicillin G, and 100 μg/mL of streptomycin (Nacalai Tesque, Inc.). Cells were incubated at 37°C in a humidified atmosphere containing 5% CO_2.

2.4 | Preparation of the conditioned medium

The conditioned medium (CM) was changed to FBS-free CM 24 h after the seeding of cells and then collected 24 h after CM exchange. The collected culture medium was centrifuged at 3500 rpm for 15 min at 4°C. The CM supernatant was collected and centrifuged at 20,000 g for 15 min at 4°C, and the supernatants were collected and passed through a 0.22 μm pore filter (Merck Millipore) and stored at 80°C.

2.5 | Animal experiments

BALB/c nu/nu female mice were purchased from CLEA Japan Inc. at 4 weeks of age and given at least 1 week to adapt to their new environment before tumor transplantation in a specific pathogen-free environment. On day 0, the mice were anesthetized with 2% isoflurane, and SK-ES-1 or A673 cells (5×10^6 cells/mouse in 100 μL total volume with DMEM suspension) were transplanted into their right hindquarters. Tumor growth was monitored once each week. Tumor resection was performed 4 weeks after transplantation. Blood samples were collected at 4 weeks after transplantation in the nonresection and control groups by cardiac puncture under anesthesia with isoflurane and collected into CAPIJECT® microcollection tubes (Terumo). Blood samples were collected 1 week after the tumor resection in the tumor resection group.

13497006, 0, Downloaded from https://onlinelibrary.wiley.com/doi/10.1111/cas.16343 by Okayama University, Wiley Online Library on [30/09/2024]. See the Terms and Conditions (https://onlinelibrary.wiley.com/terms-and-conditions) on Wiley Online Library for rules of use; OA articles are governed by the applicable Creative Commons License

2.6 | EV purification from the cell culture medium

EVs from the culture medium supernatant were purified as previously reported with partial modification.[17] Each cell line was grown to 60%–70% confluence and CM was then exchanged for FBS-free. The CM samples were collected 24 h after medium exchange and centrifuged at 3500 rpm for 15 min at 4°C, followed by further centrifugation at 9000 g for 30 min at 4°C. The collected supernatant was passed through a 0.22 μm pore filter (Merck Millipore) to remove apoptotic bodies, microvesicles, and cell debris. The supernatant was then concentrated to approximately 1 mL using 100 kDa of molecular weight cut-off ultrafiltration membranes (Fisher Scientific) at 4°C. The sample was ultracentrifuged (Optima TL-100; Beckman Coulter) at 100,000 g for 70 min at 4°C. The resulting pellet was rinsed with PBS, followed by further ultracentrifugation at 100,000 g for 70 min at 4°C. Finally, the supernatant was discarded, with EVs concentrated in the pellet. The obtained EVs were authenticated by scanning electron microscope (SEM) and an NS300 Nanosight® nanoparticle analyzer (Malvern Instruments Ltd.). These procedures were performed under the Minimal Information for Studies of Extracellular Vesicles (MISEV2023) standard.[18]

2.7 | EV purification from human and murine serum

Size exclusion chromatography on a drip using EVSecond® columns (GL Sciences Inc.) in a low-temperature environment was used to purify EVs from human and murine serum samples. The column was initially equilibrated with 700 μL of PBS twice, followed by a blocking step using 700 μL of FBS. After repeating the wash steps six times with 700 μL of PBS, the collected serum samples of 200 μL were loaded onto this column, followed by the collection of 12 consecutive fractions in 100 μL of PBS. Western blotting was used to analyze CD9 expression in these fractions. CD9-positive fractions were recognized as the EV-rich portion.[19]

2.8 | RNA extraction and RT-qPCR analysis

Total RNA was extracted from cells collected after 24 h of cell culture and EVs using the miRNeasy mini Kit (Qiagen) following the manufacturer's instructions. The PrimeScript™ RT reagent Kit (Takara) was used to generate complementary DNA from total RNA.

The primers 5′-TATAGCCAACAGAGCAGCAG-3′ (forward) and 5′-GTTGAGGCCAGAATTCATGTTA-3′ (reverse) were used to amplify EWS/Fli-1 mRNA. The appropriate amplicons of type-1 and type2 EWS/Fli-1 fusion size were 158 and 185 bp, respectively. Amplification of GAPDH mRNA was achieved with primers 5′-CATCAAGAAGGTGGTGAAGCAG-3′ (forward) and 5′-CGTCAAAGGTGGAGGAGTGG-3′ (reverse). The appropriate amplicon size was 118 bp. The PCR program consisted of enzyme activation at 95°C for 30 s followed by amplification for 40 cycles (95°C for 5 s, 62°C for 30 s). The amplified products were separated by 2% agagose gel electrophoresis.

2.9 | Liquid chromatography–mass spectrometry analysis

The purified EVs were dried and dissolved in lysis buffer (50 mM HEPES-NaOH [8.0], 12 mM deoxycholate, and 12 mM N-lauroyl sarcosinate). EV proteins (10 μg) were reduced with 20 mM tris (2-carboxyethyl) phosphine (Sigma-Aldrich) at 100°C for 10 min, followed by alkylation with 50 mM iodoacetamide (Sigma-Aldrich) at 25°C in the dark for 45 min. Samples were mixed with Laemmli's sample buffer and loaded onto a polyacrylamide sodium dodecyl sulfate gel. Electrophoresis was discontinued when the loading dye (bromophenol blue) reached 2 mm under the top of the separation gel. Coomassie brilliant blue-stained and excised protein-containing gel bands were subjected to in-gel digestion with 100 ng of Trypsin/Lys-C Mix (Promega) at 37°C for 12 h. The resulting peptides were extracted from gel fragments and analyzed using an LTQ-Orbitrap-Velos mass spectrometer (Thermo Fisher Scientific) combined with an UltiMate 3000 Rapid Separation Liquid Chromatography nanoflow high-performance liquid chromatography system (Dionex Corporation). MaxQuant software was used for protein identification and quantification analyses.[20] The tandem mass spectrometry spectra were searched against *the Homo sapiens* protein database in SwissProt, in which a false discovery rate (FDR) of 1% was set for both peptide and protein identification filters. Only "razor + unique peptides" were used to calculate the relative protein concentration.

2.10 | Immunoblot analysis

An electrophoretic gradient across Mini-PROTEAN® tris-glycine extended gels (Bio-Rad) was used for total protein from cell (10 μg) and EV (1 μg) fractionation. Loading samples were normalized according to protein concentrations quantified using the Bradford assay.[21] The gels were then transferred onto Immun-Blot® PVDF membranes (Bio-Rad) under wet electrophoretic conditions. The blotted protein was blocked for 1 h at room temperature with Odyssey® blocking buffer in PBS (Li-Cor) and was followed by incubation overnight at 4°C with the following primary antibodies: 1:200 anti-CD63 mouse monoclonal antibody (Abcam), 1:200 anti-CD81 mouse monoclonal antibody (sc-23,962; Santa Cruz Biotechnology), 1:1000 anti-cytochrome-c mouse monoclonal antibody (Abcam), 1:10,000 anti-β-actin mouse monoclonal antibody (Sigma-Aldrich), 1:500 anti-CD99 mouse monoclonal antibody (12E7, ab8855, Abcam), 1:500 anti-ENO-1 mouse monoclonal antibody (8G8; Calbiochem, Merck KgaA), and 1:500 anti-SLC1A5 rabbit polyclonal antibody (ab84903; Abcam). Thereafter, IRDye® 800CW antirabbit IgG and IRDye® 680RD antimouse IgG secondary antibodies (Li-Cor) were incubated with the protein-blotted membrane for 1 h at room temperature. The Odyssey® imaging system (Li-Cor) was used to detect fluorescence.

13497006, 0, Downloaded from https://onlinelibrary.wiley.com/doi/10.1111/cas.16343 by Okayama University, Wiley Online Library on [30/09/2024]. See the Terms and Conditions (https://onlinelibrary.wiley.com/terms-and-conditions) on Wiley Online Library for rules of use; OA articles are governed by the applicable Creative Commons License

2.11 | Sandwich ELISA

Anti-CD63 or anti-CD81 antibody (250 ng/well) was immobilized on a Nunc MaxiSorp flat-bottomed 96-well plate (Thermo Fischer Scientific) by shaking on a plate shaker at room temperature for 1 h. The blocking solution (150 μL/well of 5% bovine serum albumin [BSA] in PBS) was then added and incubated on a plate shaker at ambient temperature for 1 h. After washing three times with PBS, EV samples of 40 μL and PBS of 60 μL were loaded into the wells. After 2 h of incubation, plates were washed three times with PBS. The biotinylated anti-CD63 antibody (1:2000), biotinylated anti-CD81 antibody (1:1000), biotinylated anti-CD99 antibody (1:1000), or biotinylated anti-ENO-1 antibody (1:4000) in 1% BSA was loaded into the wells (100 μL/well). After 1 h of incubation, the plates were washed three times with PBS and then covered with 100 μL/well of SA-HRP (1:400; Abcam) in 1% BSA solution. After 45 min of incubation, plates were washed three times with PBS and covered with 100 μL/well of TMB Substrate Solution (Thermo Fischer Scientific). The reaction was stopped after 15 min of incubation using 100 μL/well of 2 N HCl. The optical density at 450 nm was immediately measured.

2.12 | Statistics and data analysis

Data are depicted as the mean ± standard deviation or the median with a 25%–75% range. The unpaired *t*-test was used to measure differences in patient demographics and clinical characteristics. Statistical differences in quantified expression levels of ELISA for targeted protein were determined using an unpaired *t*-test or followed by analysis of variance (ANOVA) Holm–Sidak's multiple comparison test. Receiver operating characteristic (ROC) curve analysis was performed to investigate the diagnostic accuracy of serum ENO-1^{+}EV levels. A two-sided *P* value of 0.05 was considered statistically significant. Statistical analyses were performed using GraphPad Prism version 6.0 (GraphPad Software).

3 | RESULTS

3.1 | Characterization of EVs secreted by ES cells

EVs secreted from ES cells and purified from the serum of healthy individuals were isolated by ultracentrifugation from the culture media of SK-ES-1, RD-ES, and A673 and by the EV-second procedure, respectively. Scanning electron microscopy revealed that these EVs appeared essentially homogeneous with a diameter of 40–100 nm, but these concentrations varied among those cell lines (Figure 1B). The size distribution was measured using Nanosight®, which revealed that the sizes of EVs derived from ES cells peaked at approximately 100 nm (Figure 1B). Furthermore, CD81-nanogold particles on the surface membrane of EVs were confirmed using transmission electron microscope (Figure 1C). Most importantly, the expression of the ES-specific fusion gene *EWSR1-FLI1* was confirmed in the collected EVs derived from the culture media of SK-ES-1, RD-ES, and A673 cells (Figure 1D). These data indicate that EVs secreted from ES cells capture the molecular characteristics of parental ES cells.

3.2 | Proteomic analysis of purified EVs from sera of patients with ES and culture media of ES cells

Proteomic analysis was performed using the EVs extracted from the serum of patients with ES pre- and posttreatment and healthy individuals ($n=4$; Table S1), and culture media of SK-ES-1, RD-ES, and A673 cell lines. EVs derived from the serum of healthy individuals were revealed to have a peak size of approximately 100 nm before proteomic analysis (Figure S1). The liquid chromatography–mass spectrometry analysis of EV samples and subsequent SwissProt database search determined approximately 950 proteins in EVs purified from human sera (FDR 1%; Table S2). Regarding the EV samples from several ES cell lines, 1321 proteins were detected in SK-ES-1-derived EVs, 1296 proteins in RD-ES-derived EVs, and 1362 proteins in A673-derived EVs. A total of 564 proteins were prominently observed in EVs from all three ES cell lines (Figure 2A). The Expression Analysis Systematic Explorer scores were calculated to elucidate the physiological functions of proteins from EVs in all three ES cell lines. The proteins detected in the ES-derived EVs were associated with nucleic acid regulation, endocytosis, and structural molecule activity (Figure 2B). Among 564 proteins prevalently detected in EVs from ES cell lines, 18 proteins consistently and potentially demonstrated expression levels on the surface of EVs from these cell lines (Figure 2C).

The proteomic analysis of EVs purified from human sera revealed 336 proteins highly expressed in ES patients before treatments compared to healthy individuals. Among these, 34 proteins are potentially expressed on the surface of EVs (Figure S2). Among these 34 proteins in EVs from human sera and 18 proteins in EVs from culture media of ES cell lines, the upregulated proteins in patients with ES compared with healthy individuals, which were reduced postoperatively, included ENO-1 and SLC1A5, known as localized proteins on the cellular membrane. CD99, a marker for the immunohistochemistry of ES, was determined as a commonly expressed protein in EVs derived from ES cell lines but was not identified in EVs purified from sera of patients with ES (Table S2).

3.3 | Identification of ENO-1 as a surface marker of EVs secreted by ES cells

We performed immunoblot analysis to investigate whether tetraspanin markers (CD63 and CD81) and the identified proteins (ENO-1, SLC1A5, and CD99) were contained in ES cell lysates and EVs secreted from ES cell lines. ENO-1 was strongly positive in ES cell lysates and EVs from all ES cell lines. CD99 was detected in all ES cell line lysates but in EVs from two of three ES cell lines. Additionally, SLC1A5 was detected in all ES cell lysates and EVs from all three ES cell lines. However, the expression levels were very low in the immunoblot

13497006, 0, Downloaded from https://onlinelibrary.wiley.com/doi/10.1111/cas.16343 by Okayama University, Wiley Online Library on [30/09/2024]. See the Terms and Conditions (https://onlinelibrary.wiley.com/terms-and-conditions) on Wiley Online Library for rules of use; OA articles are governed by the applicable Creative Commons License

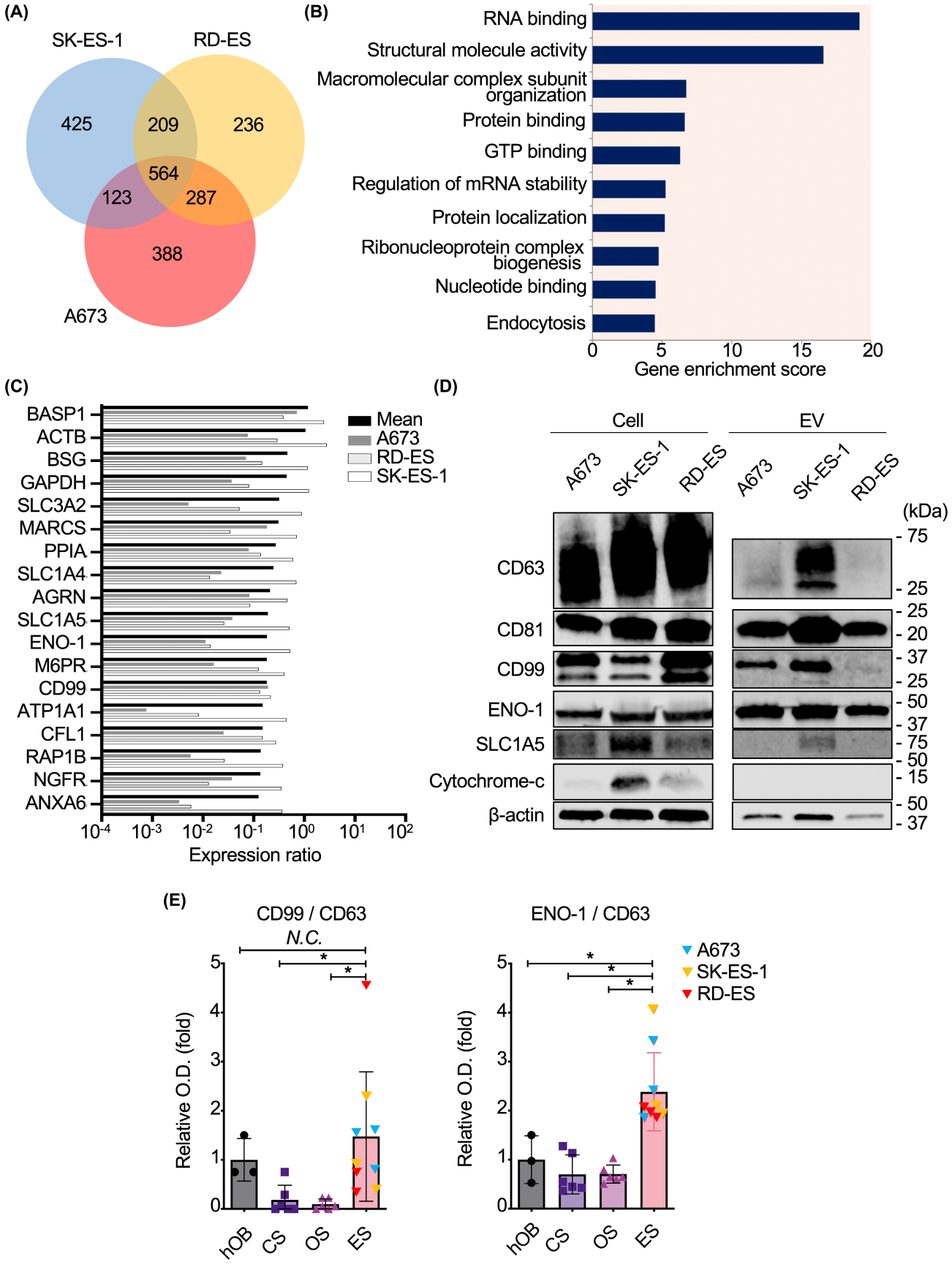

13497006, 0, Downloaded from https://onlinelibrary.wiley.com/doi/10.1111/cas.16343 by Okayama University, Wiley Online Library on [30/09/2024]. See the Terms and Conditions (https://onlinelibrary.wiley.com/terms-and-conditions) on Wiley Online Library for rules of use; OA articles are governed by the applicable Creative Commons License

FIGURE 2 Identification of ENO-1 as a surface marker protein on EVs secreted from ES cell lines. (A) Venn diagram illustrating proteomic profiling of EVs secreted from SK-ES-1, RD-ES, and A673 cell lines. A total of 2232 proteins were detected in EVs from these cell lines. (B) Expression Analysis Systematic Explorer (EASE) scores indicating the physiological functions of detected proteins from ES-derived EVs. (C) Proteins that were commonly and potentially expressed on the surface of EVs from ES cell lines. (D) ES cell lysates and ES-derived EV immune-blot analysis. ENO-1 expressions were strongly positive in all ES cell lysates and EVs from all cell lines. CD99 expressions were positive in all ES cell lysates but EVs from two of three ES cell lines. ES cell lysates and ES-derived EVs demonstrated very weak or negative SLC1A5 expressions. (E) Sandwich ELISA was used to evaluate proteomic expressions on the surface of EVs. Expressions of both CD99 and ENO-1 on the surface of ES-derived EVs were significantly higher than those from OS and CS cell lines. Only ENO-1 expression on ES-derived EVs was significantly higher than those from hOB cells. $^*P < 0.05$, one-way ANOVA. CS, chondrosarcoma; HOB, human osteoblast cells; OS, osteosarcoma. EV, extracellular vesicle.

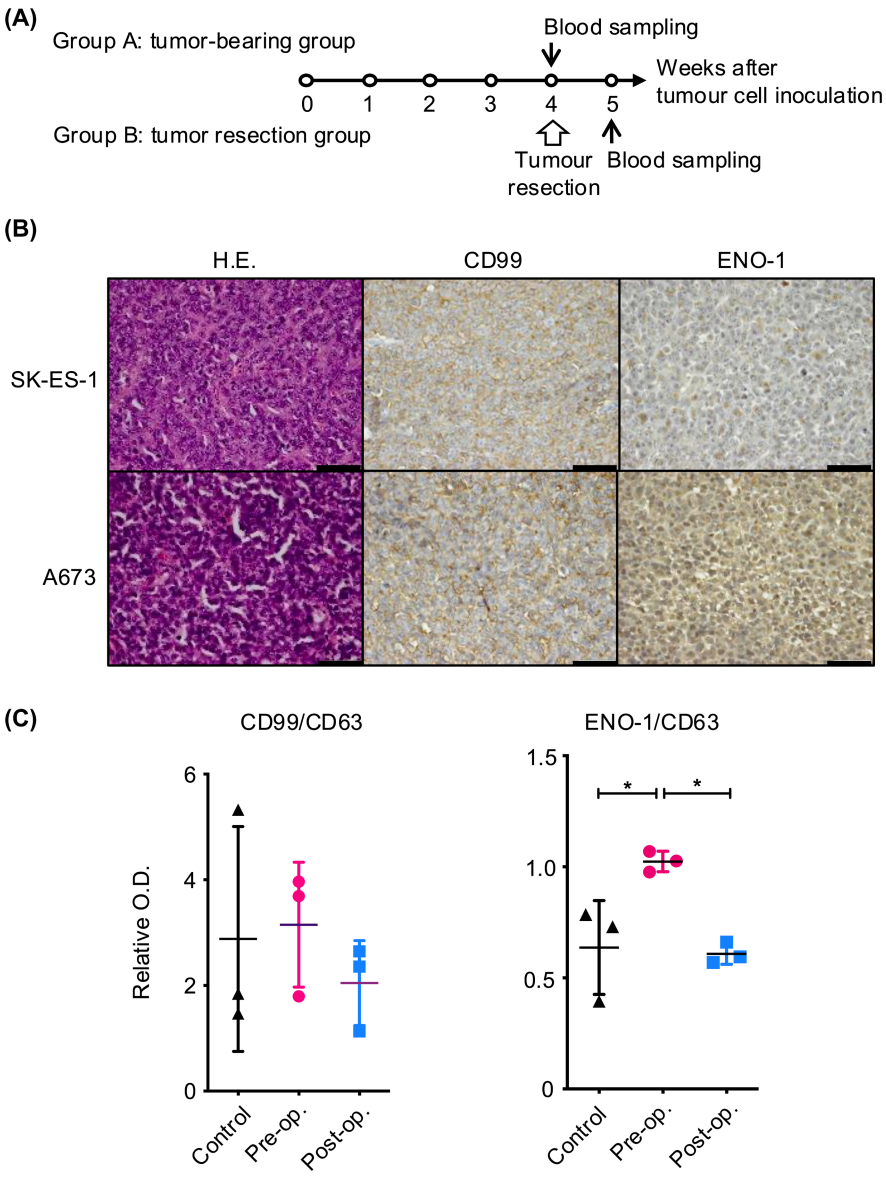

FIGURE 3 Serum CD99$^+$ EV and ENO-1$^+$ EV expression levels during tumor development in ES-bearing mice. (A) The scheme of the animal experiment is indicated. (B) Immunohistochemical analysis of SK-ES-1 and A673 tumor sections. CD99 and ENO-1 expression were moderately to strongly positive on cellular membranes. Scale bar = 50 μm. (C) CD99/CD63 and ENO-1/CD63 sandwich ELISA. CD99 was positive for EVs purified from sera of ES-bearing mice but could not distinguish tumor-bearing mice from control mice or mice after tumor resection. ENO-1 expression was significantly higher in EVs purified from sera of ES-bearing mice than in those from control mice and reduced after tumor resection. $^*P < 0.05$, one-way ANOVA. H.E.; hematoxylin and eosin.

analysis (Figures 2D and S3–S8). In contrast, ENO-1 was strongly expressed in EVs from all three ES cell lines, therefore further investigations were performed focusing on ENO-1 and CD99 expressions.

We next confirmed ENO-1 and CD99 expression on the surface of EVs from ES cells. Sandwich-based ELISA revealed that both ENO-1/CD63 and CD99/CD63 were significantly higher on the surface of ES-derived EVs than that of EVs from both OS and CS cell lines (Figure 2E). Notably, the expression levels of ENO-1/CD63 in EVs from ES cell lines were significantly higher than those in EVs from control hOB cells (Figure 2E).

13497006, 0, Downloaded from https://onlinelibrary.wiley.com/doi/10.1111/cas.16343 by Okayama University, Wiley Online Library on [30/09/2024]. See the Terms and Conditions (https://onlinelibrary.wiley.com/terms-and-conditions) on Wiley Online Library for rules of use; OA articles are governed by the applicable Creative Commons License

3.4 | *In vivo* dynamics of ES-derived circulating EVs

We evaluated possible correlations between tumor growth and circulating ES-derived EV levels using SK-ES-1 and A673 ES-bearing mice (Figure 3A). We confirmed CD99 and ENO-1 expressions in the ES tissue specimens. Immunohistochemical analysis of tumors resected from xenografted mice revealed moderate to strong ENO-1 and CD99 expressions on the cellular membrane (Figure 3B).

We then investigated ENO-1/CD63 expressions in circulating EVs in ES-bearing mice using sandwich ELISA. ENO-1/CD63 expressions were significantly higher in EVs purified from the sera of ES-bearing mice than in those from control mice ($P<0.050$; Figure 3C). Importantly, ENO-1/CD63 expressions were significantly reduced after tumor resection ($P<0.050$; Figure 3C). Conversely, CD99/CD63 was positive for EVs purified from the sera of ES-bearing mice. However, we could not distinguish ES-bearing mice from control mice using CD99/CD63 expression, and reduced CD99/CD63 expressions after tumor resection were not statistically significant (Figure 3C).

3.5 | Clinical relevance of circulating ENO-1$^+$EVs in patients with ES

We investigated ENO-1 and CD99 expressions in tumor specimens obtained from patients with ES before evaluating the clinical relevance of circulating ES-derived EVs. Both CD99 and ENO-1 expressions on cellular membranes were strongly expressed in all 16 ES tumor specimens, which was confirmed by immunohistochemical analysis (Figure 4A). We then investigated the expression levels of CD99/CD81 and ENO-1/CD81 in EVs purified from sera of 13 patients with ES and 13 healthy individuals. Tables S1 and S3 show the demographic and tumor-related characteristics of the patients. CD99/CD81 sandwich ELISA revealed similar CD99 expression among patients with ES and healthy individuals ($P=0.950$; Figure 4B). Conversely, ENO-1/CD81 sandwich ELISA revealed that ENO-1 expression was significantly higher in EVs purified from the sera of patients with ES than in EVs from healthy individuals ($P=0.007$). ROC analysis revealed that ENO-1 expression levels distinguished patients with ES from the healthy population with an area under the curve (AUC) value of 0.92 (95% confidence interval=0.83–1.0, $P=0.0002$). Using a cutoff value of 0.66, the sensitivity was 84.6% and the specificity was 84.6% (Figure 4C). Furthermore, circulating ENO-1 expression levels indicate the potential utility for tumor monitoring during the treatment course (Figure 5A–D). A 14-year-old boy with localized ES of the lumbar vertebra underwent chemotherapy and radiotherapy (Figure 5A). The circulating ENO-1 expression levels decreased after chemotherapy and radiotherapy as a curative intent. A 16-year-old girl with localized ES in the thoracic wall was treated with neoadjuvant chemotherapy, followed by surgery and adjuvant chemotherapy (Figure 5B). The circulating ENO-1 expression levels markedly decreased after neoadjuvant chemotherapy and low levels were maintained to the end of treatment protocol. A 39-year-old woman diagnosed with ES of the rib underwent neoadjuvant chemoradiation followed by surgery and adjuvant chemotherapy (Figure 5C). The circulating ENO-1 expression levels decreased

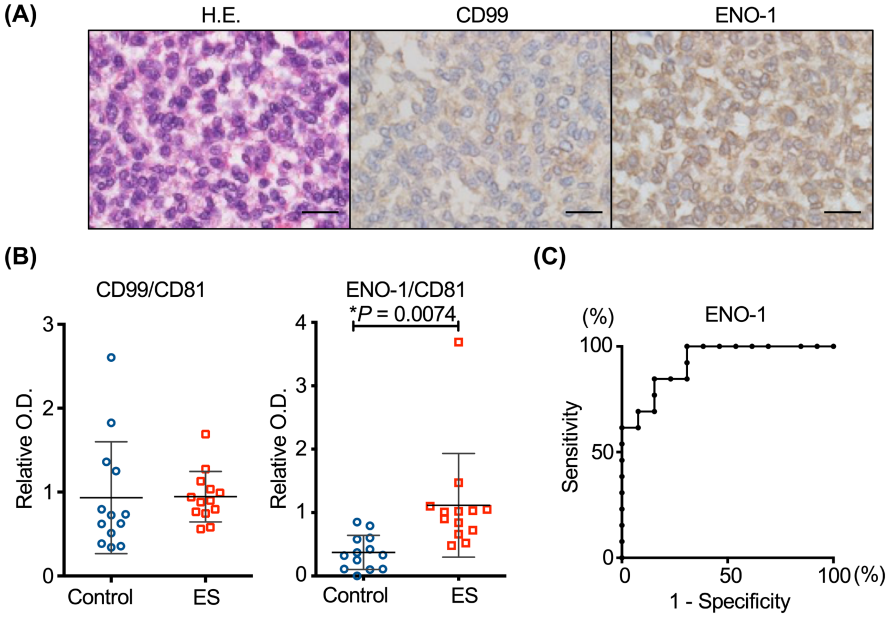

FIGURE 4 Membranous CD99 and ENO-1 expressions on circulating EVs and tissue specimens from patients with ES. (A) Immunohistochemical analysis of CD99 and ENO-1 expression on ES tumor specimens. Scale bar = 50 μm. Membranous expressions of ENO-1 were stronger than those of CD99. (B) Sandwich ELISA targeting CD99 and ENO-1. Membranous CD99 expressions on circulating EVs were comparable between patients with ES and healthy individuals ($P=0.950$), and ENO-1 expressions were significantly higher in patients with ES than those in healthy individuals (*FLI$P=0.0074$, Student's *t*-test). (C) ROC analysis. Circulating ENO-1$^+$ EV levels distinguished patients with ES from healthy individuals, with an AUC value of 0.92 ($P=0.0002$). H.E.; hematoxyline and eosin. ES; Ewing sarcoma.

13497006, 0, Downloaded from https://onlinelibrary.wiley.com/doi/10.1111/cas.16343 by Okayama University, Wiley Online Library on [30/09/2024]. See the Terms and Conditions (https://onlinelibrary.wiley.com/terms-and-conditions) on Wiley Online Library for rules of use; OA articles are governed by the applicable Creative Commons License

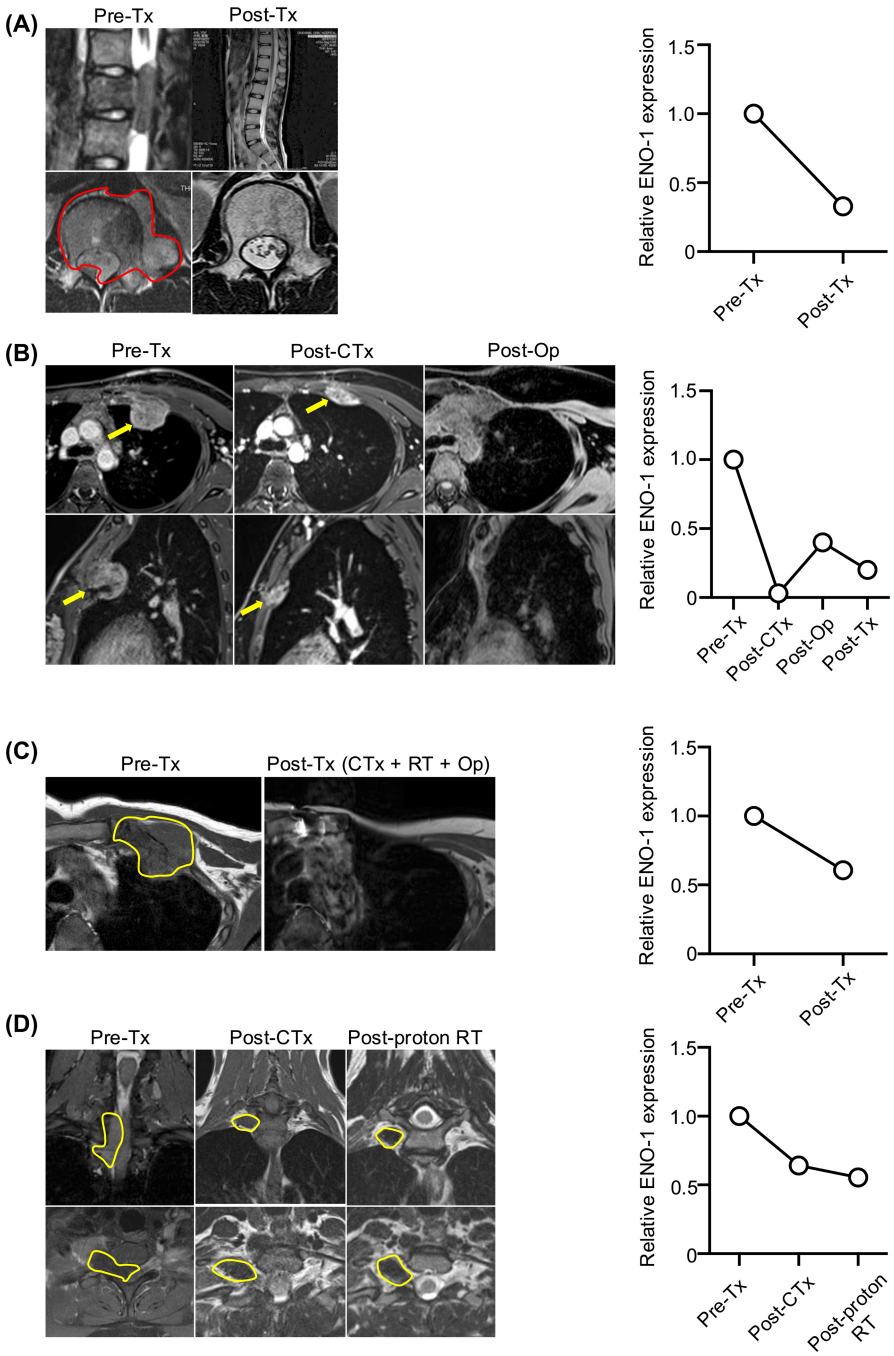

FIGURE 5 ENO-1 expression levels for monitoring tumor burden during the treatment course in patients with ES. (A) A 14-year-old boy diagnosed with ES of the lumbar vertebra underwent chemotherapy and radiotherapy as a curative intent. (B) A 16-year-old girl with ES in the thoracic wall was treated with neoadjuvant chemotherapy followed by surgical resection and adjuvant chemotherapy. (C) A 39-year-old woman diagnosed with ES of the rib underwent neoadjuvant chemoradiation followed by surgical resection and adjuvant chemotherapy. (D) A 19-year-old man diagnosed with extraskeletal ES of the thoracic vertebra underwent chemotherapy and proton radiotherapy as a curative intent. In all patients, circulating ENO-1^{+} EV levels decreased after multidisciplinary treatments or at the end of the treatment course. Tx; Treatment, CTx; Chemotherapy, Op; Operation, RT; Radiotherapy

at the end of treatment protocol. A 19-year-old man diagnosed with extraskeletal ES at the thoracic vertebra underwent chemotherapy and proton radiotherapy as a curative intent (Figure 5D). The circulating ENO-1 expression levels decreased after induction chemotherapy but further decreased after proton radiotherapy. All cases were diagnosed based on the confirmation of fusion gene by PCR analysis (Figure S9).

4 | DISCUSSION

The development of diagnosing and monitoring tumors using non-invasive methods indicates an important step in precision oncology. Methods of liquid biopsy include the detection of circulating tumor cells (CTCs), circulating cell-free nucleic acids (circulating tumor DNAs [ctDNAs], circulating cell-free DNAs [cfDNAs], and circulating cell-free microRNAs), and circulating EVs. Accumulating evidence has confirmed the advantages of each method of liquid biopsy, but the limitations of these modalities have also been documented. In particular, purifying CTCs is sometimes difficult in the early stage of the tumor because of low abundance in the bloodstream. A larger volume of blood is necessary to collect CTCs, and the collected samples are contaminated with a variety of cells other than tumor cells.[22,23] Cost-effectiveness, unsatisfactory sensitivity, and false-negative/positive detection of molecules regarding ctDNA diagnostics have been problematic because normal cfDNA gives nearly all

13497006, 0, Downloaded from https://onlinelibrary.wiley.com/doi/10.1111/cas.16343 by Okayama University, Wiley Online Library on [30/09/2024]. See the Terms and Conditions (https://onlinelibrary.wiley.com/terms-and-conditions) on Wiley Online Library for rules of use; OA articles are governed by the applicable Creative Commons License

the components of circulating DNA.[24] The advantages of the modality used in this study include reduced blood volume, lower cost, and higher sensitivity compared to ctDNA analysis. Previous reports have indicated that ctDNA analysis typically requires approximately 2 mL of plasma,[25] whereas, in our study, we were able to detect ENO-1$^+$EVs using only 700 μL of serum. Regarding cost effectiveness, ctDNA testing is estimated to range between $200 and $1400 per sample. In contrast, our method costs approximately $100 per sample. In terms of sensitivity, the sensitivity and specificity of detection of ENO-1$^+$EVs were both 84.6% (Figure 4C), whereas ctDNA was reportedly detectable in 52.1% of patients with ES.[25] Furthermore, liquid biopsy targeting circulating EVs offers the potential for tumor monitoring from early stage compared to detection of CTCs and possible applications as a drug delivery system.[13,26]

This study identified ENO-1 and CD99 as surface proteins on ES-derived EVs. CD99 is a 32-kDa cell surface glycoprotein molecule that plays an important role in cell migration, death, and differentiation.[27] CD99 is routinely used to pathologically confirm ES. ES generally shows a strong, diffuse membranous expression of CD99. *EWSR1-FLI1* regulates CD99 expression through the direct binding CD99 promoter and indirect miRNA regulation.[28–30] CD99 maintains neural differentiation of ES cells through *miR-34a-Notch*-mediated control of *NF-κB* signaling.[31,32] However, CD99 expression is not specific to ES but is found in normal tissues and other malignancies such as lymphoma and leukemia.[33] In this study, circulating CD99$^+$ EVs could not differentiate patients with ES from healthy individuals. However, membranous CD99 expression on EVs confirms that EVs carry similar molecular expression profiles to their parental ES cells.

ENO-1 is a cytoplasmic glycolytic enzyme that catalyzes phosphoenolpyruvate formation from 2-phosphoglycerate, which generates ATP during glycolysis. This molecule plays an important role as a mediator in pathological conditions such as infection, inflammation, and autoimmunity.[34,35] Recent studies revealed that ENO-1 is responsible for proliferation and metastasis in many cancer types, including non-small cell lung cancer, non-Hodgkin's lymphoma, gastric cancer, and hepatocellular carcinoma,[36–41] and is a possible target for diagnosis and anticancer therapy.[36,37,40–44] ENO-1 mainly localizes in the cytoplasm, but cytoplasmic ENO-1 is trafficked to the cell surface under inflammatory or malignant conditions, although its molecular mechanisms remain unclear.[38,42,45,46] As shown in Figures 3B and 4A, ENO-1 is robustly expressed in ES tumors, indicating the possible efficacy of ENO-1-targeted therapy. Zhong et al. reported that anti-ENO1 antibodies suppressed metastatic lung cancer by regulating the activation of hepatocyte growth factor receptor-wingless-related integration site (HGFR-WNT) signaling pathways, thereby downregulating epithelial-to-mesenchymal transition.[47] Similarly, Li et al. demonstrated that controlling ENO-1 regulated the HGFR-Akt pathway, which may overcome cancer cell proliferation and drug resistance.[48] Mohapatra et al. reported the role of the CMTM6/ENO-1/Akt signaling axis in regulation of cisplatin resistance. Knocking down CMTM6 reduced membrane ENO-1 expression and reduced the stemness properties of chemoresistant cells of esophageal cancer.[49] According to the report from Cardenas et al., ENO-1 could be a novel target for neuroendocrine-like prostate cancer (NEPC), and researchers are evaluating small molecule inhibitors that target ENO-1 in chemoresistant NEPC cells with promising initial results.[50] Notably, decreased proteomic expression of ENO-1 was identified in *EWSR1-FLI1* knockdown cells.[51] This evidence indicates that ENO-1 may serve not only as a promising circulating marker but also as a novel target for ES.

Currently, molecular detection of Friend erythroleukemia transfromation-E26 transformation-specific (FET-ETS) gene fusions or fluorescence in situ hybridization (FISH)-based detection of EWSR1 rearrangements using biopsy samples is fundamental for ES diagnosis, especially if cases have unusual clinical and pathological features. Importantly, ENO-1$^+$EVs do not have greater diagnostic value than detection of fusion genes using biopsy samples. However, tumor monitoring using the repeated biopsy is impossible in patients who are disease-free after tumor excision, and repeated biopsy in patients with advanced disease is not preferred because of its invasiveness. The reason why we recruited healthy individuals was to confirm whether the targets were tumor-specific. However, through a variety of experiments, we identified that these are useful for tumor monitoring. Our developed protocol of liquid biopsy using ENO-1$^+$EVs is suitable for monitoring tumor dynamics over time and detecting minimal residual disease for ES. Recently, an ultrasensitive method for detecting circulating EVs using ExoScreen was developed, which directly detects surface proteins on EVs without their purification.[7] This diagnostic tool detects circulating cancer-derived EVs from as little as 5 mL of serum in patients with cancer,[7] which provides more accurate tumor detection in patients with colorectal cancer than CEA and CA19-9, which are the most prominently used tumor-associated antigens in colorectal cancer management. Along with these developments, liquid biopsy using ENO-1$^+$EVs is a novel tool suitable for tumor monitoring in patients with ES.

The development of circulating biomarkers for tumor monitoring in ES could offer three advantages: detection of minimal residual disease, early detection of recurrence/metastasis, and real-time monitoring of tumor response to systemic therapy. For localized Ewing sarcoma, the vincristine, doxorubicin, cyclophosphamide-ifosphamide and etoposide (VDC-IE) regimen is increasingly recognized as the standard treatment domestically and internationally. The JESS14 clinical trial is currently ongoing to clarify the efficacy of bi-weekly VDC-IE. In the A-1 and B-2 arms where complete resection is subsequently possible, the possibility of minimal residual disease is not a major problem. However, in the A-2 and B-3 arms where surgical margins would be insufficient and thus postoperative radiotherapy is required, the possibility of minimal residual disease is a major problem. In addition, in the B-1 arm where tumor is unresectable and thus curative radiotherapy is required, we cannot evaluate whether there is a residual viable tumor or not at the end of protocol. Currently, there are no established methods to detect such residual diseases. Indeed, tissue biopsy is not recommended after curative radiotherapy. In such scenarios, evaluating circulating ENO-1$^+$ EVs could be an alternate option. If the levels of these circulating EVs do

13497006, 0, Downloaded from https://onlinelibrary.wiley.com/doi/10.1111/cas.16343 by Okayama University, Wiley Online Library on [30/09/2024]. See the Terms and Conditions (https://onlinelibrary.wiley.com/terms-and-conditions) on Wiley Online Library for rules of use; OA articles are governed by the applicable Creative Commons License

not decline at the end of protocol, further maintenance therapy or additional treatments may be warranted, which could improve survival outcomes. Currently, detection of recurrence or metastasis is primarily based on imaging diagnostics, which may not detect micrometastasis of the tumor. However, if circulating ENO-1$^+$EVs levels are elevated, closer follow-up with imaging diagnostics may accurately detect recurrence or metastasis at an earlier stage. If patients had lung metastasis, surgical intervention is possible if the number of metastatic lesions is limited. For metastatic ES, treatment efficacy is usually evaluated through imaging diagnostics, usually performed at intervals of several weeks. By assessing circulating EVs, it may be possible to monitor the real-time response to the treatment, which may be helpful in reconsidering the treatment strategy.

In conclusion, we determined ENO-1 as a surface marker of ES-derived EVs by proteomic profiling using ES cell supernatants and sera from patients with ES. Detecting circulating ENO-1$^+$EVs could be a novel method for evaluating the real-time treatment response, detecting residual tumors after treatments, and discovering recurrent tumors early in ES management.

AUTHOR CONTRIBUTIONS

Koji Uotani: Formal analysis; investigation; writing – original draft. **Tomohiro Fujiwara:** Conceptualization; funding acquisition; supervision; writing – original draft. **Koji Ueda:** Investigation; methodology; resources. **Aki Yoshida:** Data curation; writing – review and editing. **Shintaro Iwata:** Resources. **Takuya Morita:** Investigation. **Masahiro Kiyono:** Investigation. **Toshiyuki Kunisada:** Data curation. **Ken Takeda:** Data curation. **Joe Hasei:** Data curation. **Yusuke Yoshioka:** Methodology; resources; writing – review and editing. **Takahiro Ochiya:** Conceptualization; methodology; writing – review and editing. **Toshifumi Ozaki:** Conceptualization.

ACKNOWLEDGMENTS

The authors thank all patients who agreed to this study project. We also thank the Central Research Laboratory of the Okayama University Medical School for the technical support for the extraction and validation of EVs.

FUNDING INFORMATION

This work is supported by the JSPS Kakenhi Grant No. 22H03202.

CONFLICT OF INTEREST STATEMENT

Koji Ueda and Takahiro Ochiya are editorial board members of Cancer Science. The other authors have no COI.

DATA AVAILABILITY STATEMENT

All data generated or analyzed during this study are included in this published article and its Supporting Information files.

ETHICS STATEMENT

Approval of the research protocol by an Institutional Reviewer Board: Okayama University Hospital (#949) and Chiba Cancer Centre Hospital (#27–30).

Informed Consent: Informed consent was obtained from each patient.

Registry and the Registration No. of the study/trial: N/A.

Animal Studies: Animal experiments were performed in accordance with the Animal Care and Use Committee at Okayama University.

ORCID

Koji Uotani https://orcid.org/0000-0002-5594-1292
Tomohiro Fujiwara https://orcid.org/0000-0003-4257-9180
Koji Ueda https://orcid.org/0000-0001-9066-4959
Shintaro Iwata https://orcid.org/0000-0002-2024-514X
Takahiro Ochiya https://orcid.org/0000-0002-0776-9918

REFERENCES

1. Pishas KI, Lessnick SL. Recent advances in targeted therapy for Ewing sarcoma. *F1000Res*. 2016;5:1-11.
2. Potratz J, Dirksen U, Jürgens H, Craft A. Ewing sarcoma: clinical state-of-the-art. *Pediatr Hematol Oncol*. 2012;29:1-11.
3. Pretz JL, Barysauskas CM, George S, et al. Localized adult Ewing sarcoma: favorable outcomes with alternating vincristine, doxorubicin, cyclophosphamide, and Ifosfamide, etoposide (VDC/IE)-based multimodality therapy. *Oncologist*. 2017;22:1265-1270.
4. Gaspar N, Hawkins DS, Dirksen U, et al. Ewing sarcoma: current management and future approaches through collaboration. *J Clin Oncol*. 2015;33:3036-3046.
5. van Niel G, D'Angelo G, Raposo G. Shedding light on the cell biology of extracellular vesicles. *Nat Rev Mol Cell Biol*. 2018;19:213-228.
6. Yoshioka Y, Konishi Y, Kosaka N, Katsuda T, Kato T, Ochiya T. Comparative marker analysis of extracellular vesicles in different human cancer types. *J Extracell Vesicles*. 2013;2:1-9.
7. Yoshioka Y, Kosaka N, Konishi Y, et al. Ultra-sensitive liquid biopsy of circulating extracellular vesicles using ExoScreen. *Nat Commun*. 2014;5:3591.
8. Mathivanan S, Ji H, Simpson RJ. Exosomes: extracellular organelles important in intercellular communication. *J Proteome*. 2010;73:1907-1920.
9. Alzhrani GN, Alanazi ST, Alsharif SY, et al. Exosomes: isolation, characterization, and biomedical applications. *Cell Biol Int*. 2021;45:1807-1831.
10. Jia S, Zhang R, Li Z, Li J. Clinical and biological significance of circulating tumor cells, circulating tumor DNA, and exosomes as biomarkers in colorectal cancer. *Oncotarget*. 2017;8:55632-55645.
11. Jia Y, Chen Y, Wang Q, et al. Exosome: emerging biomarker in breast cancer. *Oncotarget*. 2017;8:41717-41733.
12. Jia Y, Yu L, Ma T, et al. Small extracellular vesicles isolation and separation: current techniques, pending questions and clinical applications. *Theranostics*. 2022;12:6548-6575.
13. Tatischeff I. Current search through liquid biopsy of effective biomarkers for early cancer diagnosis into the rich cargoes of extracellular vesicles. *Int J Mol Sci*. 2021;22:1-26.
14. Brock G, Castellanos-Rizaldos E, Hu L, Coticchia C, Skog J. Liquid biopsy for cancer screening, patient stratification and monitoring. *Transl Cancer Res*. 2015;4:280-290.
15. Melo SA, Luecke LB, Kahlert C, et al. Glypican-1 identifies cancer exosomes and detects early pancreatic cancer. *Nature*. 2015;523:177-182.
16. Kunisada T, Miyazaki M, Mihara K, et al. A new human chondrosarcoma cell line (OUMS-27) that maintains chondrocytic differentiation. *Int J Cancer*. 1998;77:854-859.
17. Wolfers J, Lozier A, Raposo G, et al. Tumor-derived exosomes are a source of shared tumor rejection antigens for CTL cross-priming. *Nat Med*. 2001;7:297-303.

13497006, 0, Downloaded from https://onlinelibrary.wiley.com/doi/10.1111/cas.16343 by Okayama University, Wiley Online Library on [30/09/2024]. See the Terms and Conditions (https://onlinelibrary.wiley.com/terms-and-conditions) on Wiley Online Library for rules of use; OA articles are governed by the applicable Creative Commons License

18. Welsh JA, Goberdhan DCI, O'Driscoll L, et al. Minimal information for studies of extracellular vesicles (MISEV2023): from basic to advanced approaches. *J Extracell Vesicles*. 2024;13:e12404.
19. Kowal J, Arras G, Colombo M, et al. Proteomic comparison defines novel markers to characterize heterogeneous populations of extracellular vesicle subtypes. *Proc Natl Acad Sci USA*. 2016;113:E968-E977.
20. Cox J, Mann M. MaxQuant enables high peptide identification rates, individualized p.p.b.-range mass accuracies and proteome-wide protein quantification. *Nat Biotechnol*. 2008;26:1367-1372.
21. Bradford MM. A rapid and sensitive method for the quantitation of microgram quantities of protein utilizing the principle of protein-dye binding. *Anal Biochem*. 1976;72:248-254.
22. Crowley E, Di Nicolantonio F, Loupakis F, Bardelli A. Liquid biopsy: monitoring cancer-genetics in the blood. *Nat Rev Clin Oncol*. 2013;10:472-484.
23. Punnoose EA, Atwal S, Liu W, et al. Evaluation of circulating tumor cells and circulating tumor DNA in non–small cell lung cancer: association with clinical endpoints in a phase II clinical trial of pertuzumab and erlotinib. *Clin Cancer Res*. 2012;18:2391-2401.
24. Pi C, Zhang M-f, Peng X-x, Zhang Y-c, Xu C-r, Zhou Q. Liquid biopsy in non-small cell lung cancer: a key role in the future of personalized medicine? *Expert Rev Mol Diagn*. 2017;17:1089-1096.
25. Shulman DS, Klega K, Imamovic-Tuco A, et al. Detection of circulating tumour DNA is associated with inferior outcomes in Ewing sarcoma and osteosarcoma: a report from the Children's oncology group. *Br J Cancer*. 2018;119:615-621.
26. Chung IM, Rajakumar G, Venkidasamy B, Subramanian U, Thiruvengadam M. Exosomes: current use and future applications. *Clin Chim Acta*. 2020;500:226-232.
27. Schenkel AR, Mamdouh Z, Chen X, Liebman RM, Muller WA. CD99 plays a major role in the migration of monocytes through endothelial junctions. *Nat Immunol*. 2002;3:143-150.
28. Franzetti G, Laud-Duval K, Bellanger D, Stern M, Sastre-Garau X, Delattre O. MiR-30a-5p connects EWS-FLI1 and CD99, two major therapeutic targets in Ewing tumor. *Oncogene*. 2013;32:3915-3921.
29. Rocchi A, Manara MC, Sciandra M, et al. CD99 inhibits neural differentiation of human Ewing sarcoma cells and thereby contributes to oncogenesis. *J Clin Invest*. 2010;120:668-680.
30. Amaral AT, Manara MC, Berghuis D, et al. Characterization of human mesenchymal stem cells from Ewing sarcoma patients. Pathogenetic implications. *PLoS One*. 2014;9:e85814.
31. Ventura S, Aryee DN, Felicetti F, et al. CD99 regulates neural differentiation of Ewing sarcoma cells through miR-34a-notch-mediated control of NF-κB signaling. *Oncogene*. 2016;35:3944-3954.
32. De Feo A, Sciandra M, Ferracin M, et al. Exosomes from CD99-deprived Ewing sarcoma cells reverse tumor malignancy by inhibiting cell migration and promoting neural differentiation. *Cell Death Dis*. 2019;10:471-485.
33. Ambros IM, Ambros PF, Strehl S, Kovar H, Gadner H, Salzer-Kuntschik M. MIC2 is a specific marker for Ewing's sarcoma and peripheral primitive neuroectodermal tumors. Evidence for a common histogenesis of Ewing's sarcoma and peripheral primitive neuroectodermal tumors from MIC2 expression and specific chromosome aberration. *Cancer*. 1991;67:1886-1893.
34. Montes A, Dieguez-Gonzalez R, Perez-Pampin E, et al. Particular association of clinical and genetic features with autoimmunity to citrullinated α-enolase in rheumatoid arthritis. *Arthritis Rheum*. 2011;63:654-661.
35. Didiasova M, Schaefer L, Wygrecka M. When place matters: shuttling of enolase-1 across cellular compartments. *Front Cell Dev Biol*. 2019;7:61.
36. Fu QF, Liu Y, Fan Y, et al. Alpha-enolase promotes cell glycolysis, growth, migration, and invasion in non-small cell lung cancer through FAK-mediated PI3K/AKT pathway. *J Hematol Oncol*. 2015;8:22-34.
37. Zhou J, Zhang S, Chen Z, He Z, Xu Y, Li Z. CircRNA-ENO1 promoted glycolysis and tumor progression in lung adenocarcinoma through upregulating its host gene ENO1. *Cell Death Dis*. 2019;10:885-898.
38. Zhu X, Miao X, Wu Y, et al. ENO1 promotes tumor proliferation and cell adhesion mediated drug resistance (CAM-DR) in non-Hodgkin's lymphomas. *Exp Cell Res*. 2015;335:216-223.
39. Chen JMM, Chiu SC, Chen KC, Huang YRJ, Liao YTA, Yu CTR. Enolase 1 differentially contributes to cell transformation in lung cancer but not in esophageal cancer. *Oncol Lett*. 2020;19:3189-3196.
40. Yang T, Shu X, Zhang H-W, et al. Enolase 1 regulates stem cell-like properties in gastric cancer cells by stimulating glycolysis. *Cell Death Dis*. 2020;11:870-882.
41. Zhu W, Li H, Yu Y, et al. Enolase-1 serves as a biomarker of diagnosis and prognosis in hepatocellular carcinoma patients. *Cancer Manag Res*. 2018;10:5735-5745.
42. Qiao G, Wu A, Chen X, Tian Y, Lin X. Enolase 1, a moonlighting protein, as a potential target for cancer treatment. *Int J Biol Sci*. 2021;17:3981-3992.
43. Zhao M, Fang W, Wang Y, et al. Enolase-1 is a therapeutic target in endometrial carcinoma. *Oncotarget*. 2015;6:15610-15627.
44. Hoang AT, Vizio B, Chiusa L, et al. Impact of tissue enolase 1 protein overexpression in esophageal cancer progression. *Int J Med Sci*. 2021;18:1406-1414.
45. Capello M, Ferri-Borgogno S, Cappello P, Novelli F. α-Enolase: a promising therapeutic and diagnostic tumor target. *FEBS J*. 2011;278:1064-1074.
46. Didiasova M, Zakrzewicz D, Magdolen V, et al. STIM1/ORAI1-mediated Ca2+ influx regulates Enolase-1 exteriorization. *J Biol Chem*. 2015;290:11983-11999.
47. Zhong Y, Li H, Li P, et al. Exosomes: a new pathway for cancer drug resistance. *Front Oncol*. 2021;11:743556.
48. Li HJ, Ke FY, Lin CC, et al. ENO1 promotes lung cancer metastasis via HGFR and WNT signaling-driven epithelial-to-mesenchymal transition. *Cancer Res*. 2021;81:4094-4109.
49. Mohapatra P, Shriwas O, Mohanty S, et al. CMTM6 drives cisplatin resistance by regulating Wnt signaling through the ENO-1/AKT/GSK3beta axis. *JCI Insight*. 2021;6:e143643.
50. Cardenas C. Glycolytic enzyme Enolase-1 (ENO-1) as a novel target for neuroendocrine-like prostate cancer: a review of up-to-date research and future prospects. *Clin Oncol Case Rep*. 2023;6(7):2.
51. Gurpide JM, Martin DH. Proteomic profiling of Ewing sarcoma reveals a role for TRAF6 in proliferation and ribonucleoproteins/RNA processing. *J Proteomics Bioinform*. 2016;9:166-175.

SUPPORTING INFORMATION

Additional supporting information can be found online in the Supporting Information section at the end of this article.

How to cite this article: Uotani K, Fujiwara T, Ueda K, et al. Identification of ENO-1 positive extracellular vesicles as a circulating biomarker for monitoring of Ewing sarcoma. *Cancer Sci*. 2024;00:1-12. doi:10.1111/cas.16343

13497006, 0, Downloaded from https://onlinelibrary.wiley.com/doi/10.1111/cas.16343 by Okayama University, Wiley Online Library on [30/09/2024]. See the Terms and Conditions (https://onlinelibrary.wiley.com/terms-and-conditions) on Wiley Online Library for rules of use; OA articles are governed by the applicable Creative Commons License